Original Article
OBESITY BIOLOGY AND INTEGRATED PHYSIOLOGY

Obesity

Bile Diversion Improves Metabolic Phenotype Dependent on Farnesoid X Receptor (FXR)

Joseph F. Pierre[1,2], Yuxin Li[3]*, Charles K. Gomes[2], Prahlad Rao[2], Eugene B. Chang[1], and Deng Ping Yin[3]*

Objective: The current study investigated whether bile diversion (BD) improves metabolic phenotype under farnesoid X receptor (FXR) deficiency.
Methods: BD was performed in high-fat diet (HFD)-fed FXR knockout (FXRko) and wild-type (WT) animals. Metabolic phenotypes, circulating enteroendocrine hormones, total bile acids (BAs) and BA composition, and cecal gut microbiota were analyzed.
Results: FXR-deficient mice were resistant to HFD-induced obesity; however, FXR-deficient mice also developed hyperglycemia and exhibited increased liver weight, liver steatosis, and circulating triglycerides. BD increased circulating total BAs and taurine-b-muricholic acid, which were in line with normalized hyperglycemia and improved glucose tolerance in HFD-fed WT mice. FXR deficiency also increased total BAs and taurine-b-muricholic acid, but these animals remained hyperglycemic. While BD improved metabolic phenotype in HFD-fed FXRko mice, these improvements were not as effective as in WT mice. BD increased liver expression of fibroblast growth factor 21 and peroxisome proliferator-activated receptor γ coactivator-1β and elevated circulating glucagon-like peptide-1 levels in WT mice but not in FXRko mice. FXR deficiency altered gut microbiota composition with a specific increase in phylum Proteobacteria that may act as a possible microbial signature of some diseases. These cellular and molecular changes in FXRko mice may contribute to resistance toward improved metabolism.
Conclusions: FXR signaling plays a pivotal role in improved metabolic phenotype following BD surgery.

Obesity (2019) **0**, 1-10. doi:10.1002/oby.22440

Introduction

Mounting evidence has suggested that the beneficial effects of bariatric surgery, such as Roux-en-Y gastric bypass and vertical sleeve gastrectomy (VSG), may be associated with or induced by increases of circulating bile acids (BAs) (1-3). We previously demonstrated that delivery of BAs to the distal intestine using bile diversion (BD) surgery improved high-fat diet (HFD)-induced obesity, insulin resistance, and energy expenditure in wild-type (WT) mice (4). The metabolic benefits induced by BD are associated with increased circulating BAs and with reconfiguration of the gut microbiota community structure (4).

BAs are dual-purpose molecules that serve digestive and hormone functions. From a hormone standpoint, they modulate glucose and lipid homeostasis acting through their receptors, the farnesoid X receptor (FXR) and G protein-coupled bile acid receptor 1 (TGR5), which play an important role in maintaining glucose homeostasis (5-7). Activation of TGR5 promotes release of glucagon-like peptide-1 (GLP-1), which reduces gastrointestinal motility and exerts strong glucose-dependent insulinotropic and glucagonostatic actions on the pancreatic β-cells (8-11). Activation of FXR reveals the following two contradictory characteristics: improving insulin release and sensitivity (12,13) and promoting obesity and diabetes (14,15). FXR activation stimulates glycogen synthesis, decreases gluconeogenesis, and increases glycolysis, resulting in improved glucose tolerance and insulin sensitivity (13,16,17). FXR signaling also exerts strong insulinotropic actions on the pancreatic β-cells and is considered a molecular mediator of the metabolic benefits of bariatric surgery (12,18). A previous report showed that activation of FXR regulated TGR5 to release GLP-1, and serum GLP-1 levels were reduced in FXR-deficient mice (19). However, FXR promotes the expression of ceramide, which mediates a variety of cellular signaling events, resulting in enhanced mitochondrial permeability

[1] Department of Medicine, University of Chicago, Chicago, Illinois, USA [2] Department of Pediatrics, University of Tennessee Health Science Center, Memphis, Tennessee, USA [3] Department of Surgery, University of Chicago, Chicago, Illinois, USA. Correspondence: Deng Ping Yin (dyin@surgery.bsd.uchicago.edu).

Funding agencies: This work was supported in part by the Clinical and Translational Science Award (CTSA) grant (CTSA TR000430) to DPY, NIH grants P30DK42086 (Digestive Diseases Research Core Center) and DK097268 to EBC, and NIH grant DK020595 to the Metabolic Core at the University of Chicago.
Disclosure: The authors declared no conflicts of interest.
Author contributions: JFP and YL contributed to most *in vitro* and *in vivo* experiments; CG and PR contributed to bile acid analyses; EBC contributed to the design of the experiment; and DPY designed and wrote the manuscript. All authors approved the final version.
*Joseph F. Pierre and Yuxin Li contributed equally to this work.
Additional Supporting Information may be found in the online version of this article.
Received: 3 October 2018; **Accepted:** 19 January 2019; **Published online 1 April 2019. doi:10.1002/oby.22440**

and inflammatory responses in the intestine. Accordingly, intestinal inhibition of FXR may reduce ceramide production and improve β-cell function (20). In addition, the FXR antagonist taurine-b-muricholic acid (TbMCA) was shown to be effective in improving obesity-associated metabolic parameters (21).

In the current study, we tested whether the global lack of FXR influences BD-induced metabolic alterations, including body weight and glucose homeostasis, enteroendocrine hormones and adipokines, BA synthesis, and microbiota composition. Accordingly, our data support the finding that FXR-deficient mice are resistant to HFD-induced obesity. However, despite being leaner, mice lacking FXR display elevated blood glucose levels compared with WT on HFD. While BD surgery increases circulating total BAs and TbMCA, which induces metabolic benefit in WT mice, FXR-deficient mice fail to respond to BD, despite elevated circulating total BAs and increased TbMCA both at baseline and following BD surgery when compared with WT. Our findings suggest that FXR is required for improved metabolic phenotype following BD surgery.

Methods

Mice and surgery

Age-matched FXR knockout (FXRko) mice and their WT littermate male mice purchased from Jackson Laboratory (Bar Harbor, Maine) were used in the current study. Mice were fed a HFD (fat calories 60%; Bio-Serv, Flemington, New Jersey) or low-fat control diet (LFD) (fat calories 11%; Bio-Serv). Four groups were designed, with 5 mice per group for LFD feeding and 10 mice per group for HFD feeding. After 8 weeks of diet feeding, five HFD-fed mice in each group underwent BD surgery, and the other five mice were used as controls. These mice were housed in the Animal Resources Center at the University of Chicago in a specific pathogen-free, temperature-controlled environment with a 12-hour light-dark cycle. The BD surgery was performed in HFD-fed mice under general anesthesia with isoflurane plus equal O_2 through a cone placed around the mouse's nose as described in previous reports (4,22). In brief, these procedures require the anastomosis of the gallbladder to the distal jejunum at a 10-cm distance (BD) to the suspensory ligament of the duodenum. The surgical success rate was 100%, and there were no mice that died of the BD procedure. After the completion of surgery, mice had free access to HFD and water and were administered buprenorphine (0.1 mg/kg) and meloxicam (1.0 mg/kg) followed by meloxicam treatment (1.0 mg/kg) every 24 hours for 3 days. At 8 weeks following surgery (the end point), tissues were collected under ketamine/xylazine anesthesia. All protocols were approved by Institutional Animal Care and Use Committee at the University of Chicago.

Analysis of metabolic phenotype

Blood glucose level was measured using a blood glucose meter (Accu-Chek Compact Plus, Roche Diabetes Care, Inc., Indianapolis, Indiana). Oral gavage glucose tolerance tests (OGTT) were performed. Briefly, mice were fasted for 4 hours prior, and blood was sampled from the tail vein for glucose tests using the same glucose meter before and at 15, 30, 60, 90, and 120 minutes after oral gavage of dextrose (20%) at 2.0 mg/g body weight.

Body weight and diet consumption were analyzed every day up to the end point. Metabolic analysis of energy balance was carried out using metabolic cages (TSE Systems, Chesterfield, Missouri), as previously described (23). Mice were placed individually in a TSE Labmaster system for 4 days, and food and water intake, physical activity, and O_2 uptake and CO_2 production were analyzed after a 2-day acclimation. The system was calibrated according to manufacturer's instructions prior to the start of the experiment.

Circulating ghrelin, GLP-1, gastric inhibitory peptide (GIP), leptin, resistin, and plasminogen activator inhibitor-1 (PAI-1) were analyzed using a Bio-Plex Pro mouse diabetes immunoassay (Bio-Rad, Hercules, California) according to manufacturer's instructions.

Quantitative real-time reverse transcription-polymerase chain reaction for mRNA analysis

The tissues were collected and immediately placed in TRIzol Reagent (Ambion, Austin, Texas). Total RNA was obtained and was reverse-transcribed to complementary DNA using the Transcriptor First Strand cDNA Synthesis Kit (Roche) according to the manufacturer's instructions. Reverse transcription-polymerase chain reaction (RT-PCR) amplification consisted of an initial denaturation step (95°C for 10 minutes), 45 cycles of denaturation (95°C for 10 seconds), annealing (55°C for 20 seconds), and extension (60°C for 30 seconds), followed by a final incubation at 55°C for 30 seconds and cooling at 40°C for 30 seconds. All measurements were normalized by the expression of *GAPDH* gene that was considered a stable housekeeping gene, as described in our previous report (4).

Total BAs and BA composition analyses

Total BAs were quantified via enzymatic assay (Crystal Chem, Downers Grove, Illinois) in peripheral according to the manufacturer's instructions. BA compositions were analyzed as in our previous report (4). Briefly, stock solutions of individual BAs and nordeoxycholic acid were prepared in methanol at a concentration of 5.0 μg/mL. Calibration standards were prepared by adding individual BAs at a concentration range of 12 ng/mL to 1.5 μg/mL to charcoal-stripped human serum. A total of 1.6 μL of nordeoxycholic acid was added to 40 μL of standards and samples. Deproteinization was carried out by adding 15 volumes of ice-cold methanol to 40 μL of standards and samples. The samples were vortexed three times for 10 seconds each and stored at –20°C for 20 minutes. The supernatant was transferred to a new tube, evaporated under vacuum, and dissolved in 100 μL of 50% methanol. The tubes were centrifuged at 11,000*g* for 1 minute before transfer into specific vials for injection into a liquid chromatography-tandem mass spectrometry system. Data were acquired on an AB Sciex triple quadrupole mass spectrometer (AB Sciex LLC, Framingham, Massachusetts) in negative ion mode coupled with a Nexera XR high-performance liquid chromatography (HPLC) system (Shimadzu Corp., Kyoto, Japan). Chromatographic separation was carried out on an Accucore XL C8 column (4 μm, 100 mm × 3 mm inner diameter; Thermo Fisher Scientific, Waltham, Massachusetts). The oven temperature was set at 50°C. Separation was carried out over a gradient of 18 minutes with 28% organic phase at 0 minutes to 90% organic phase at 18 minutes. Quantitation of BAs was carried out on MultiQuant Software version 3.0.2 (AB Sciex LLC).

Cecal content microbiota analysis

Gut microbiota in the cecal content were analyzed as described in our previous report (4). Briefly, primers specific for the 16S ribosomal RNA (rRNA) V4-V5 region (forward 515F: 5'-GTGYCAGCMGCCGCGGTAA-3' and reverse 806R: 5'-GGACT-

ACHVGGGTWTCTAAT-3') that contained Illumina 3' adapter sequences (Illumina Inc., San Diego, California) as well as a 12-base pair barcode were used. Sequences were generated by an Illumina MiSeq DNA platform at Argonne National Laboratory (Lemont, Illinois) and analyzed by the program Quantitative Insights into Microbial Ecology (QIIME) (24). Operational Taxonomic Units (OTUs) were picked at 97% sequence identity using open reference OTU picking against the Greengenes database (25). Representative sequences were aligned via PyNAST, taxonomy was assigned using the RDP Classifier, and a phylogenetic tree was built using FastTree, all performed in QIIME (1.9).

Pathological examination

Selected naive HFD-fed and BD-treated mice were sacrificed, and the livers were collected for pathological examinations (hematoxylin and eosin) at 8 weeks post surgery. Significant lesions included steatosis, ballooning, and intracinar and portal inflammation, and the lesions were graded as mild (1+, up to 33%), moderate (2+, 33%-66%), and severe (3+, > 66%).

In vitro and *in vivo* studies of activation of FXR signaling

Inflammatory responses are mediated through inflammatory signaling pathways, such as nuclear factor-κB (NF-κB), causing tumor necrosis factor α (TNFα) expression. To test whether the FXR agonist chenodeoxycholic acid (CDCA) inhibited NF-κB activity and TNFα expression in macrophages, bone marrow-derived macrophages (BMDMs) transfected with a luciferase gene under the control of the NF-κB promoter were incubated with lipopolysaccharide (0.025 μg/mL), free fatty acid (FFA) (palmitic acid, 0.1 μm), and CDCA (1.0 μm; MilliporeSigma, Burlington, Massachusetts). BMDMs were maintained in DMEM (Invitrogen, Carlsbad, California) supplemented with 10% fetal calf serum (FCS) at 37°C in a 5% CO_2 incubator for 4 hours. NF-κB activity was tested by luciferase assay (Promega, Madison, Wisconsin) and TNFα by quantitative RT-PCR. To test whether activation of FXR improved obesity and glucose tolerance, chenodeoxycholic acid was administered to HFD-fed WT mice at a dose of 150 mg/kg (dissolved in 100 μL of 1% carboxymethylcellulose) by oral gavage daily for 4 weeks. The same dose of lithocholic acid (LCA) was administered to HFD-fed WT mice by oral gavage daily for 4 weeks (26).

Statistical analysis

Sequence reads were analyzed using QIIME. Significant changes in OTU abundance were assessed using Kruskal-Wallis test (false discovery rate correction $P \leq 0.05$). Differences between groups in microbiota phylum and genus levels were analyzed by Kruskal-Wallis. All other comparisons were calculated using ANOVA tests (StatView version 4.5; Abacus Concepts, Berkeley, California), and $P < 0.05$ was considered significant. The results are presented as mean ± SEM.

Results

BD improves body weight and glucose tolerance in FXRko mice but not as effectively as in WT mice

The current study examined whether BD surgery improves obesity and glucose tolerance in the absence of FXR compared with WT mice. Figure 1 shows no statistical differences in body weight between LFD-fed WT and LFD-fed FXRko animals ($P > 0.05$; Figure 1A, body weight in grams and Figure 1B, body weight as percentage). However, HFD-fed FXRko mice displayed significantly lower body weight at 8 weeks on HFD feeding compared with HFD-fed WT mice (FXRko vs. WT, $P < 0.05$; Figure 1A-1B), suggesting that mice lacking FXR are resistant to HFD-induced obesity. These findings set the stage to determine whether FXR mediates the metabolic benefits induced by BD in age-matched WT and FXRko mice fed HFD for 8 weeks. We observed that BD significantly reduced body weight (Figure 1C, body weight in grams and Figure 1D, body weight as percentage) and fat mass (epididymal white adipose tissue, Figure 1E-1F) in HFD-fed WT and HFD-fed FXRko animals. Liver weight from age-matched LFD-fed FXRko mice exhibited a marked increase compared with WT mice; however, absolute liver weight (in grams) was not significantly changed in HFD-fed FXRko mice because of resistance to diet-induced obesity (Figure 1G). The ratio of liver to body weight was elevated in LFD-fed and BD-treated FXRko mice compared with WT mice (Figure 1H).

Blood glucose and OGTT were measured in WT and FXRko mice after fasting 4 hours. Fasting blood glucose levels were significantly increased in age-matched FXRko mice following 8 weeks of LFD or HFD feeding compared with WT animals (FXRko-LFD vs. WT-LFD, $P < 0.001$; FXRko-HFD vs. WT-HFD, $P = 0.05$; Figure 2A). However, there were no differences in response to OGTT across groups (Figure 2B-2C). The current data suggest that mice lacking FXR develop chronic hyperglycemia and maintain normal glucose tolerance. BD improved HFD-induced hyperglycemia in HFD-fed WT and HFD-fed FXRko mice; however, blood glucose was maintained at higher levels in FXRko mice (≈200 mg/dL; Figure 2D). BD resulted in a better outcome in improving glucose tolerance in HFD-fed WT mice than in HFD-fed FXRko mice (WT-BD vs. FXRko-BD, $P = 0.004$; Figure 2E-2F). These findings collectively show that BD does not significantly improve hyperglycemia and glucose tolerance in the absence of FXR.

FXR is required for hepatic responses after BD surgery

Mice lacking FXR revealed enlarged liver (Figure 1F), liver steatosis with moderate (LFD-fed) and severe (HFD-fed) structural damage (Figure 3A), and increased circulating triglycerides in LFD-fed FXRko mice (Figure 3B), consistent with previous findings linking FXRko and lipid dysregulation (27). While HFD-fed WT mice were characterized by the accumulation of lipid droplets, HFD-fed FXRko livers displayed many microscopic lipid droplets (Figure 3A). Following BD, liver steatosis improved in HFD-fed WT mice but was largely unchanged in FXRko animals, in which the abundance of small lipid vesicles was visible in all samples. Fibroblast growth factor 21 (FGF21), a member of the fibroblast growth factor family of signaling molecules, plays an important role in protecting against obesity-induced hepatic metabolic stress by enhancing fatty acid oxidation and tricarboxylic acid cycle flux. The pathogenesis of liver steatosis and nonalcoholic fatty liver disease was shown to involve dysregulation of peroxisome proliferator-activated receptor α (PPARα) and FGF21 (28). Our prior work demonstrated that increased primary BAs following BD promoted expression of FGF21, PPARα, and peroxisome proliferator-activated receptor γ coactivator 1-β (PGC-1β) in the livers of HFD-fed WT mice (4). Consistently, the current study found that BD significantly increased hepatic FGF21 gene expression in HFD-fed WT mice; however, this was not observed in FXRko mice (Figure 3C). PGC-1β is a nuclear receptor that was shown to regulate fatty acid oxidation and protect against liver steatosis (29). In earlier work, PGC-1β also

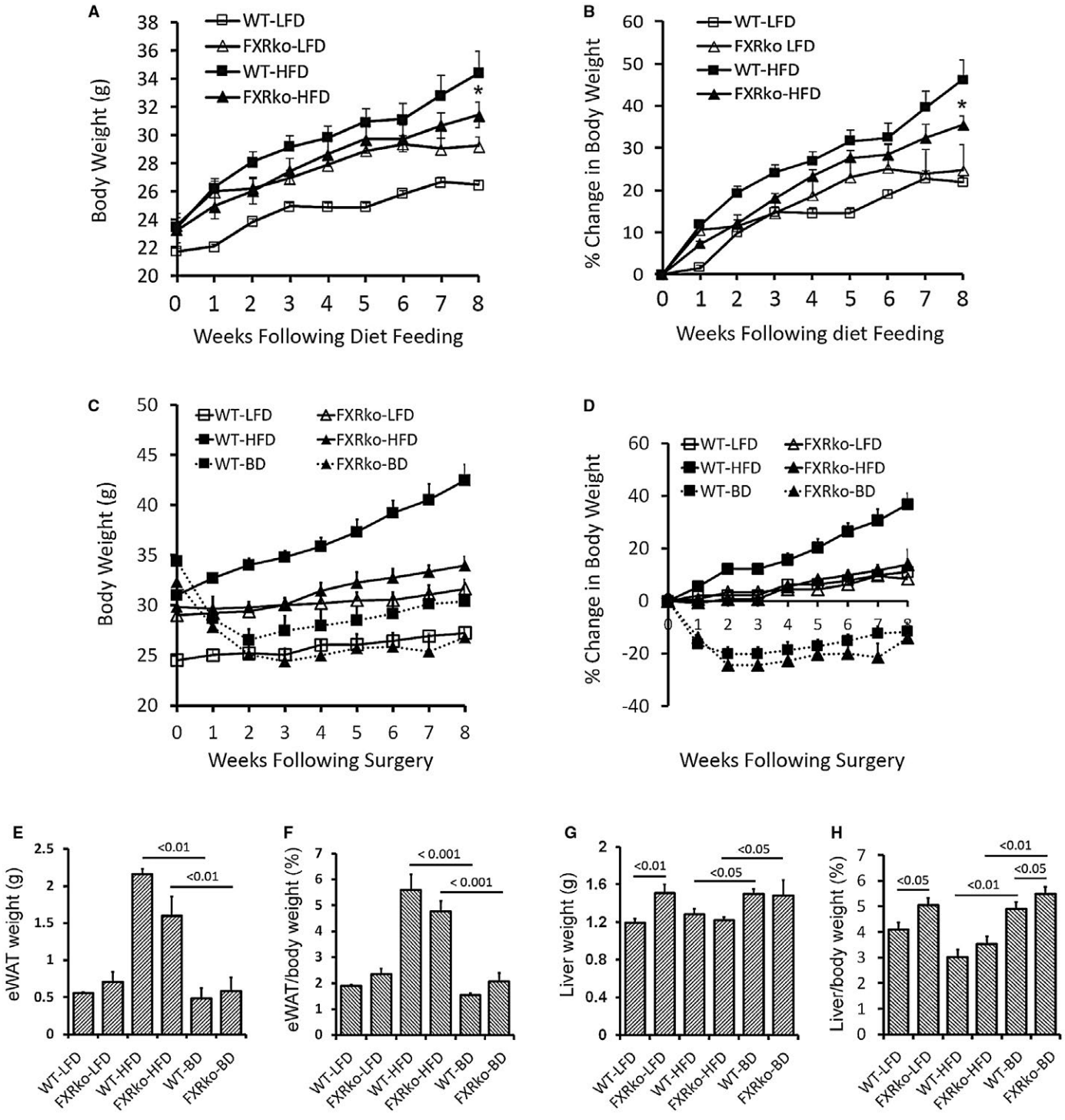

Figure 1 Animals lacking FXR are resistant to diet-induced obesity, but liver weight is increased. (**A**) Body weight changes in grams in LFD-fed (n = 5 each group) and HFD-fed (n = 10 each group) WT and FXRko mice before BD surgery. *FXRko HFD vs. WT HFD, $P < 0.05$. (**B**) Body weight changes as percentages in LFD-fed and HFD-fed WT and FXRko mice before BD surgery. FXRko HFD vs. WT HFD, $P < 0.05$ (n = 5 each group). (**C**) BD reduced body weight (in grams) in both HFD-fed WT and FXRko mice (n = 5 each group). (**D**) BD reduced body weight (as percentage) in both HFD-fed WT and FXRko mice. (**E**) BD reduced fat mass (epididymal white adipose tissue [eWAT] in grams) in both HFD-fed WT and FXRko mice. WT HFD vs. WT BD, $P < 0.001$; and FXRko HFD vs. FXRko BD, $P < 0.001$. (**F**) BD reduced fat mass (eWAT as percentage) in both HFD-fed WT and FXRko mice. (**G**) Liver weight in grams. Liver weight was significantly increased in LFD-fed and BD-treated FXRko mice. WT LFD vs. FXRko LFD, $P < 0.01$; and WT BD and FXRko BD vs. WT HFD and FXRko HFD, $P < 0.05$. (**H**) Ratios of liver/body weight as percentages. WT LFD vs. FXRko LFD, $P < 0.05$; WT BD and FXRko BD vs. WT HFD and FXRko HFD, $P < 0.01$.

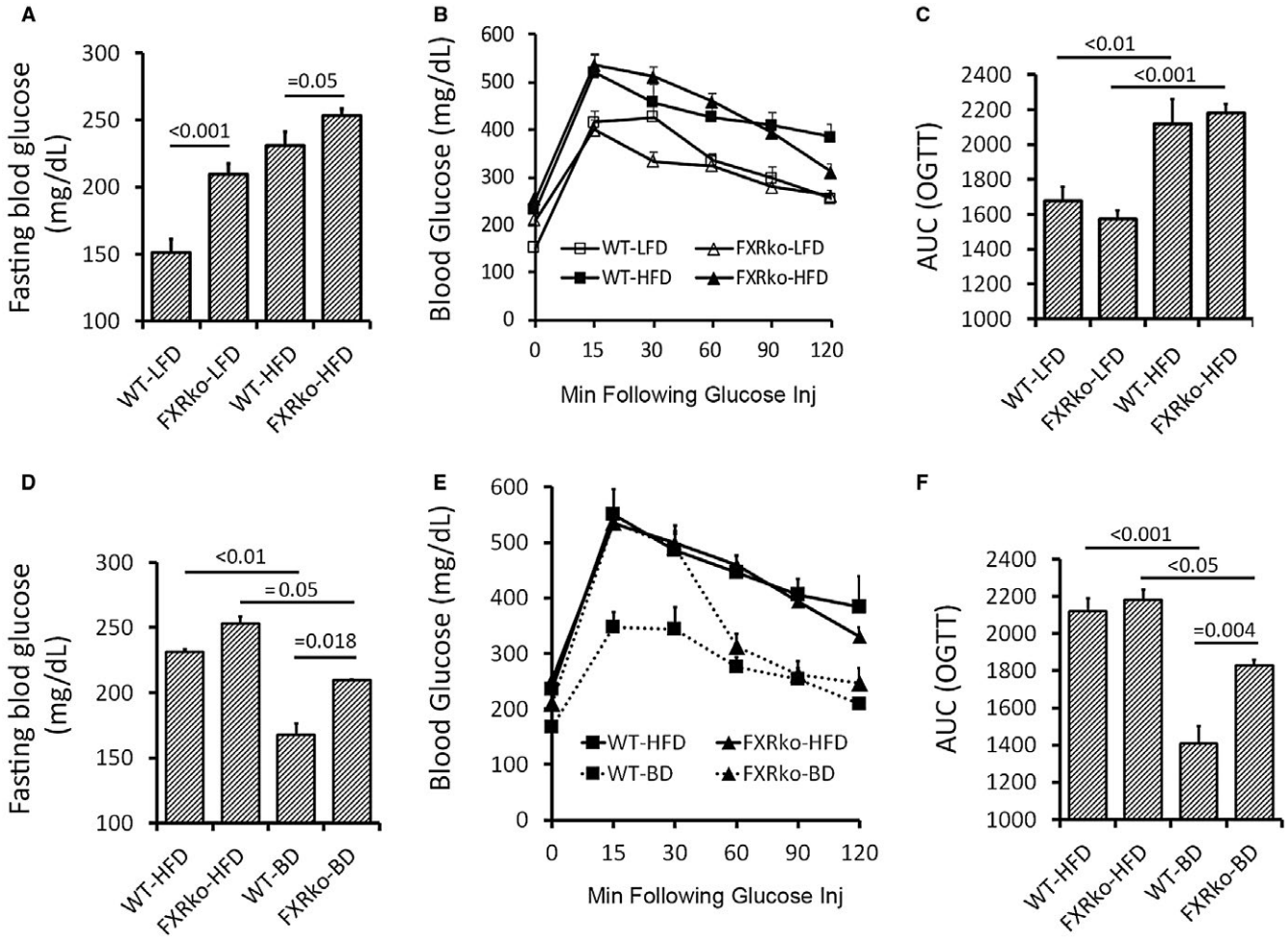

Figure 2 BD improves hyperglycemia and glucose tolerance in WT mice but not in FXRko mice (n = 5 each group). (**A**) LFD-fed FXRko mice developed hyperglycemia. Fasting blood glucose levels, WT LFD vs. FXRko LFD, $P < 0.001$; WT HFD vs. FXRko HFD, $P = 0.05$. (**B**) HFD impaired OGTT in both WT and FXRko mice. (**C**) Areas under curve (AUC) of OGTT. (**D**) BD decreases fasting blood glucose levels in HFD-fed WT ($P < 0.01$) and in HFD-fed FXRko mice ($P = 0.05$). However, WT BD vs. FXRko BD, $P = 0.018$. (**E**) BD improved glucose tolerance in HFD-fed WT and HFD-fed FXRko mice. (**F**) AUC of OGTT. WT HFD vs. WT BD, $P < 0.001$; FXRko HFD vs. FXRko BD, $P < 0.05$; WT BD vs. FXRko BD, $P = 0.004$.

mediated diet-induced changes in FGF21 gene expression, whereas FGF21 induced and activated PPARα (30). HFD reduced expression of PGC-1β in WT and FXRko mice. BD significantly increased PGC-1β expression in the livers of WT mice, but BD failed to promote PGC-1β in FXRko animals (Figure 3D). Interestingly, PPARα expression was elevated in LFD-fed and HFD-fed FXRko mice but decreased following BD surgery in these animals. In contrast, BD promoted PPARα expression in WT mice compared with baseline levels observed under LFD and HFD feeding (Figure 3E).

Lack of FXR alters expression of endocrine hormones and adipokines

BD promoted an increase in serum GLP-1 in WT animals (WT-BD vs. WT-LFD and WT-HFD, $P < 0.0001$; Figure 4A), which is consistent with previous work (4). Although BD increased the average level of GLP-1 in HFD-fed FXRko mice, GLP-1 levels in WT mice were significantly higher than FXRko mice ($P < 0.05$; Figure 4A). HFD promoted leptin expression, which is associated with increased fat mass, and BD reduced leptin production in HFD-fed WT mice. However, leptin was not significantly increased in HFD-fed FXRko mice (Figure 4B), indicating a resistance to diet-induced obesity. HFD elevated resistin, and BD reduced resistin, but this was not statistically significant ($P > 0.05$; Figure 4C). We observed reduced ghrelin levels in HFD-fed WT and HFD-fed FXRko mice, and while BD reversed this, this was not significant ($P > 0.05$; Figure 4D). Finally, there were no differences in GIP and PAI-1 across all groups ($P > 0.05$; Figure 4E-4F).

Lack of FXR alters BA and gut microbiota homeostasis

To test whether the lack of FXR alters BA synthesis and composition, we analyzed circulating total BAs and BA composition. Total BAs were increased in LFD-fed mice (FXRko-LFD vs. WT-LFD, $P < 0.01$) and BD-treated FXRko mice (FXRko-BD vs. WT-BD, $P < 0.01$). TbMCA was increased in HFD-fed FXRko mice (FXR-HFD vs. WT-HFD, $P < 0.05$) and BD-treated WT mice (WT-BD vs. WT-HFD, $P < 0.01$) (Supporting Information Figure S1).

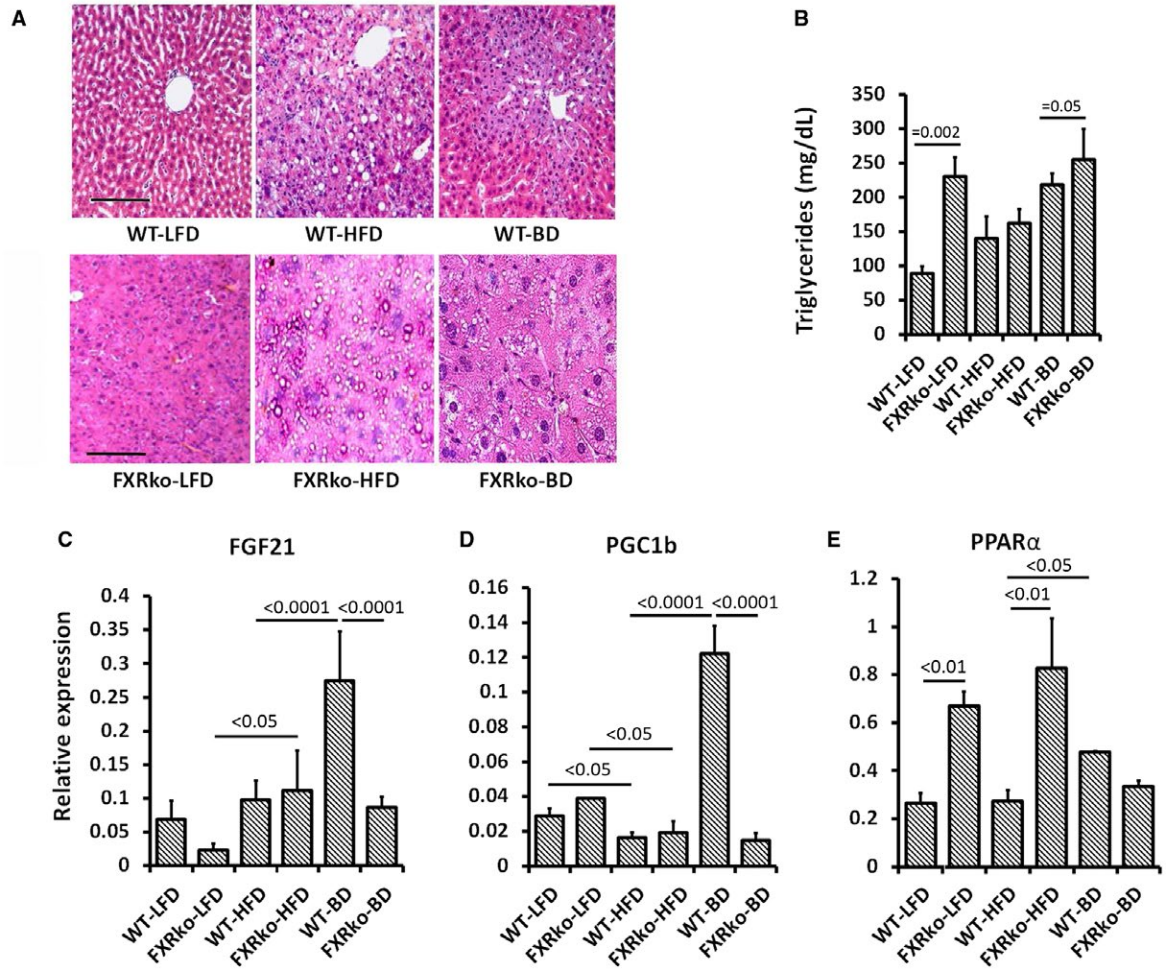

Figure 3 Liver hematoxylin and eosin staining, circulating triglyceride levels, and hepatic gene expression. (**A**) BD improved HFD-induced liver steatosis in HFD-fed WT mice but not in HFD-fed FXRko mice. (**B**) Circulating triglyceride levels. FXRko LFD vs. WT LFD mice, $P = 0.002$; WT BD vs. FXRko BD, $P = 0.05$. (**C**) Liver FGF21 gene expression. FXRko LFD vs. FXRko HFD, $P < 0.05$; WT HFD vs. WT BD and WT BD vs. FXRko BD, $P < 0.0001$. (**D**) Liver PGC-1β expression. WT HFD and FXRko HFD vs. WT LFD and FXRko LFD, $P < 0.05$; WT HFD vs. WT BD and WT BD vs. FXRko BD, $P < 0.0001$. (**E**) Liver PPARα expression. WT LFD vs. FXRko LFD, $P < 0.01$; WT HFD vs. FXRko HFD, $P < 0.01$; WT HFD vs. WT BD, $P < 0.05$.

To examine whether FXRko influences gut microbiota composition, cecal contents were collected for next-generation sequencing, targeting the 16S rRNA V4-V5 region at 8 weeks post surgery. Unweighted analysis distinguishes differences in rare taxa, as absolute abundance is ignored. This analysis suggests these treatment conditions select for distinct microbial community membership. Figure 5A demonstrates that LFD-fed FXRko mice clustered distinctly from LFD-fed WT mice (left upper panels), and HFD-fed FXRko and BD-treated FXRko mice clustered distinctly from WT mice (right upper and right lower panels). Shannon diversity analysis showed decreased diversity in HFD-fed WT, HFD-fed FXRko, and BD-treated WT mice but not in BD-treated FXRko mice (Figure 5B). The phyla Firmicutes and Bacteroidetes showed differences across LFD-fed and HFD-fed WT and FXRko animals (Figure 5C-5D, 5F-5G). Interestingly, Proteobacteria was significantly increased in LFD-, HFD-, and BD-treated FXRko mice (Figure 5E, 5H, 5K). At the genus level, the lack of FXR decreased *Bacteroides* (in LFD- and HFD-fed FXRko mice) and *Lactobacillus* (in LFD-fed and BD-treated FXRko mice) and increased family Desulfovibrionaceae in all LFD- and HFD-fed and BD-treated FXRko animals (Supporting Information Figure S2).

To test whether the lack of FXR influences BA conversion, we analyzed predictive gene orthologues from the 16S data for bacterial-derived bile salt hydrolase (BSH) and 7α-hydroxysteroid dehydrogenase (7α-HSDH). The results showed a decrease of BSH abundance in LFD-fed and BD-treated FXRko mice (Supporting Information Figure S3A). In contrast, 7α-HSDH abundance was significantly increased in LFD-fed, HFD-fed, and BD-treated FXRko mice (Supporting Information Figure S3B).

Activation of FXR inhibits inflammatory reaction and improves glucose tolerance

Activation of FXR has been shown to inhibit inflammatory reactions (31,32). We tested whether the FXR agonist CDCA attenuates

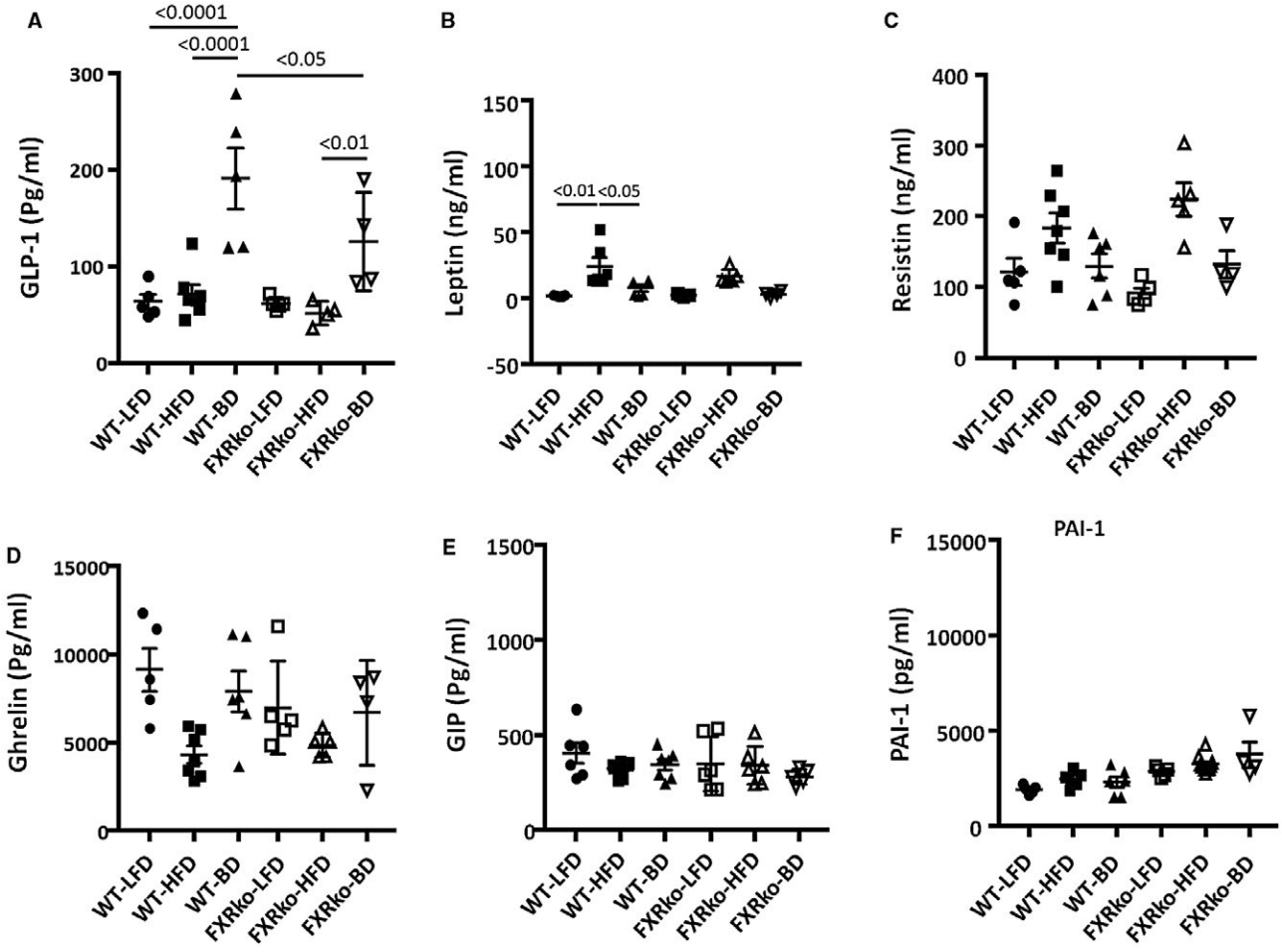

Figure 4 Circulating endocrine hormones. (**A**) BD significantly increased circulating GLP-1. WT BD vs. WT LFD and WT HFD, $P < 0.0001$; FXRko HFD vs. FXRko BD, $P < 0.05$; WT BD vs. FXRko BD, $P < 0.05$. (**B**) HFD enhanced circulating leptin levels in HFD-fed WT mice but not in HFD-fed FXRko mice. WT LFD vs. WT HFD, $P < 0.01$; WT HFD vs. WT BD, $P < 0.05$. (**C**) BD decreased circulating resistin in both HFD-fed WT and FXRko mice, but it was not statistically significant ($P > 0.05$). (**D-F**) There were no statistical differences among groups ($P > 0.05$). $n = 5$ per group.

inflammatory response and improves metabolic phenotype. In the BMDM culture, FFA increased luciferase activity, indicating increased NF-κB activity, which was inhibited by additional CDCA (Figure 6A). TNFα mRNA was elevated by the stimulation of FFA but also inhibited by CDCA (Figure 6B). The results showed that the treatment with CDCA, but not LCA or vehicle, improved glucose tolerance (Figure 6C-6D).

Discussion

The beneficial effects of bariatric surgery, such as Roux-en-Y gastric bypass and VSG, may be associated with delivery of BAs to the distal intestine and increases of circulating BAs that trigger downstream signaling pathways via the activation of BA receptors (1-3). Consistent with our previous report (4), current findings demonstrate that delivery of BAs to the distal intestine by BD improves metabolic phenotype in HFD-fed WT mice. Mice lacking FXR diverged from WT mice with the following two contradictory characteristics: resistance to HFD-induced obesity associated with increased PPARα and the development of hyperglycemia along with increased circulating total BAs and TbMCA. Previous findings demonstrated that the absence of FXR reduced the ability of VSG to improve body weight and glucose tolerance (12). The current study shows that BD improves hyperglycemia, glucose tolerance, and liver steatosis in HFD-fed WT mice in concert with significant increases of circulating GLP-1 levels and liver FGF21 gene expression in HFD-fed WT mice. However, while BD surgery improved hyperglycemia and glucose tolerance in HFD-fed FXRko mice, these improvements were not as marked compared with HFD-fed WT mice, suggesting FXR, in part, mediates the metabolic benefits of BD.

BAs are synthesized from cholesterol in the liver, and the rate-limiting enzyme CYP7A1 initiates the classic pathway of BA synthesis, which is regulated by FXR. The absence of FXR increases BA synthesis characterized by increased circulating primary BAs, including TbMCA. BD delivers BAs to the distal intestine where increased TbMCA inhibits FXR and may contribute to improved metabolic phenotype, including reduced body weight, fat mass, and energy expenditure (33). However,

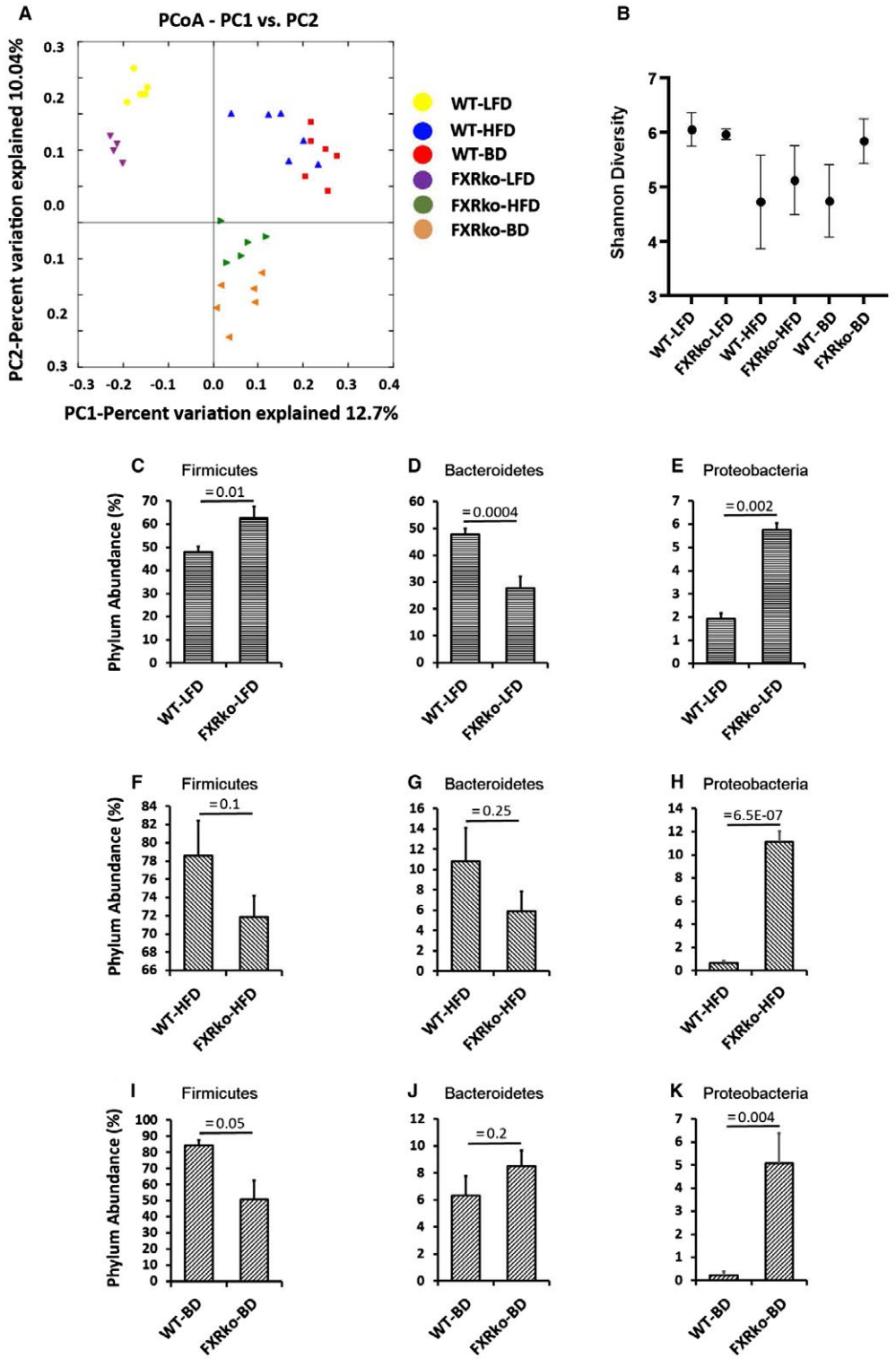

Figure 5 Lack of FXR altered gut microbiota composition (n = 5 per group). (**A**) Weighted UniFrac analysis of beta diversity. (**B**) Shannon analysis of microbiome diversity. **(C)** Phylum Firmicutes in LFD-fed mice. WT LFD vs. FXRko, $P = 0.01$. (**D**) Phylum Bacteroidetes in LFD-fed mice. WT LFD vs. FXRko LFD, $P = 0.0004$. (**E**) Phylum Proteobacteria in LFD-fed mice. WT LFD vs. FXRko LFD, $P = 0.002$. **(F)** Phylum Firmicutes in HFD-fed mice. WT HFD vs. FXRko HFD, $P = 0.1$. (**G**) Phylum Bacteroidetes in HFD-fed mice. WT HFD vs. FXRko HFD, $P = 0.25$. **(H)** Phylum Proteobacteria in HFD-fed mice. WT HFD vs. FXRko HFD, $P = 6.5E\text{-}07$. (**I**) Phylum Firmicutes in BD-treated mice. WT BD vs. FXRko BD, $P = 0.05$. (**J**) Phylum Bacteroidetes in BD-treated mice. WT BD vs. FXRko BD, $P = 0.2$. (**K**) Phylum Proteobacteria in BD-treated mice. WT BD vs. FXRko BD, $P = 0.004$.

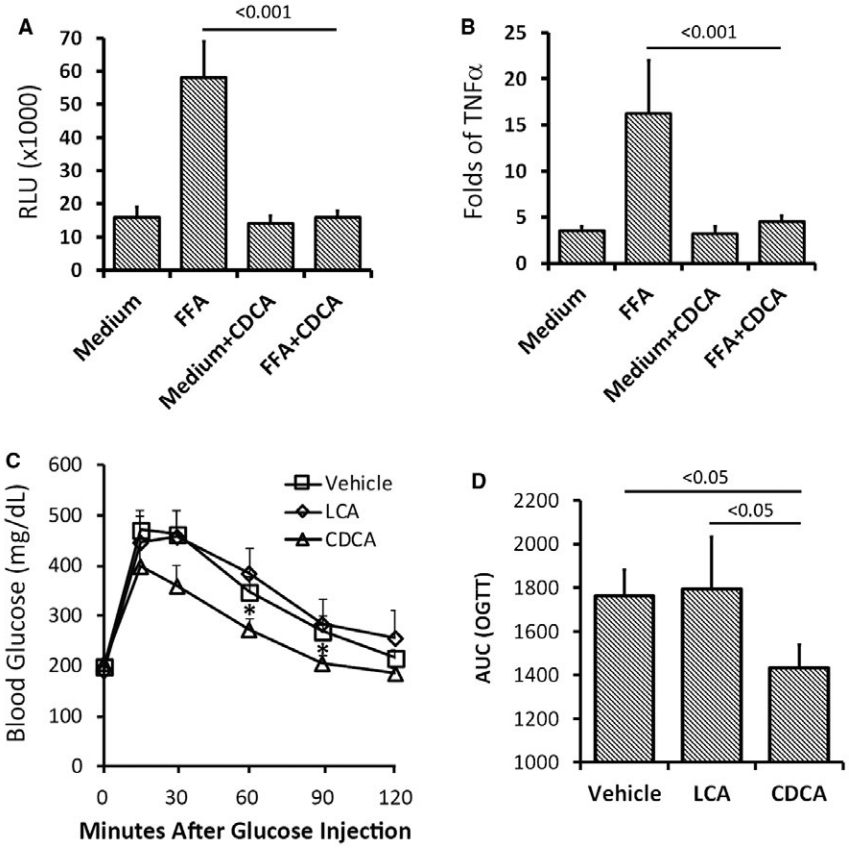

Figure 6 FXR agonist CDCA inhibited inflammatory responses and improved glucose tolerance (n = 5 per group). (**A**) CDCA inhibited FFA-induced NF-κB activity in BMDM culture. FFA+CDCA vs. FFA, $P < 0.001$. (**B**) CDCA inhibited TNFα expression in BMDM culture. FFA+CDCA vs. FFA, $P < 0.001$. (**C,D**) CDCA improved glucose tolerance in HFD-fed WT mice. CDCA vs. vehicle and LCA, $P < 0.05$. RLU, relative luminescence unit.

increased TbMCA does not improve hyperglycemia and glucose tolerance in HFD-fed FXRko mice, indicating dependency on FXR signaling. Hepatic deficiency of FXR was shown to contribute to lipid accumulation in the liver (34), whereas impaired FXR signaling in β-cells influenced insulin release (35). Previous reports have suggested that activation of FXR inhibits or promotes GLP-1 secretion (19,36). Our results show that while BD results in increases in circulating GLP-1 in both HFD-fed WT mice and HFD-fed FXRko mice, GLP-1 levels are significantly higher in WT mice than FXRko mice, which is consistent with previous findings that FXR may work in concert with TGR5 in promoting GLP-1 secretion (19). Reduced GLP-1 secretion may also contribute to reduced metabolic response in global FXR deficiency following BD surgery.

In the intestine, BAs and the microbiota reciprocally control their compositional profile. HFD was shown to induce increased phylum Firmicutes or the Firmicutes/Bacteroidetes ratio, whereas BD surgery enhanced Bacteroidetes in WT mice (4). Recent findings showed that FXR activation altered gut microbiota composition in humans (37). The current data show a distinct distribution of cecal microbiota in LFD- and HFD-fed FXRko mice with a decrease of phylum Bacteroidetes. Within *Bacteroides*, the relative abundance of bacteroides was decreased in LFD-fed and HFD-fed FXRko mice. More interestingly, the lack of FXR led to an increase in the phylum Proteobacteria that was shown to produce lipopolysaccharide and act as a possible microbial signature of diseases, including metabolic disorders (38). Within the phylum Proteobacteria, the relative abundance of the Gram-negative bacteria family Desulfovibrionaceae was increased in FXR animals, which may contribute to intestinal inflammation (39). BAs are deconjugated by bacterial-derived BSH as the first step in the generation of secondary BAs. Subsequently, the action of bacterial 7α-HSDH on deconjugation results in the production of secondary BAs (40). Our findings show that the lack of FXR results in a reduction of bacteroides-derived BSH and an increase in 7α-HSDH that catalyze the bioconversion of cholic acid and CDCA to 7-oxo-DCA and 7-oxo-LCA, respectively, consistent with a previous report (18). 7α-HSDH are widespread among members of Firmicutes-derived genera *Clostridium*, *Eubacterium*, *Bacteroides*, or *Escherichia* (41,42).

FXR agonists have been utilized as therapy for obesity and diabetes in rodents (43) and in humans (44). However, a previous report indicated that FXR agonists decreased energy expenditure and induced obesity and insulin resistance in mice (15). Our data show that FXR agonist CDCA inhibits FFA-induced NF-κB activity and TNFα expression *in vitro* and

improves glucose tolerance *in vivo*. One major limitation of our findings relates to the evidence that human and mouse BA composition is markedly different; i.e., primary BAs in humans include cholic acid and CDCA conjugated with glycine, whereas mice also produce MCA species conjugated with taurine (TaMCA and TbMCA). It has been shown that CDCA is an FXR agonist, whereas TbMCA is an FXR antagonist (45). Consequently, the extrapolation of BA-related results in mice must be carefully interpreted concerning human implications. Another limitation of this study is that using a global knockout of FXR cannot differentiate the tissue-specific effects of FXR activity or modulation. However, taken together, this work demonstrates an important role for FXR in the regulation of BA homeostasis, energy balance, and glucose metabolism.

In conclusion, these findings demonstrate that mice lacking FXR are resistant to HFD-induced obesity associated with increased PPARα. However, the absence of FXR also leads to hyperglycemia and dysregulation of BA and microbiota homeostasis. While BD improves body weight and glucose tolerance in FXRko mice, it is not as effective in WT mice. Finally, the FXR agonist CDCA inhibits FFA-mediated NF-κB activity and TNFα expression *in vitro* and improves glucose tolerance in HFD-fed WT mice. Our results contribute to the understanding of the mixed metabolic phenotypes observed in global FXR knockouts and provide the potential to develop tissue-specific FXR manipulations for the treatment of obesity and type 2 diabetes.

References

1. Schauer PR, Bhatt DL, Kirwan JP, et al. Bariatric surgery versus intensive medical therapy for diabetes: 3-year outcomes. *New Engl J Med* 2014;370:2002-2013.
2. Thoni V, Pfister A, Melmer A, et al. Dynamics of bile acid profiles, GLP-1, and FGF19 after laparoscopic gastric banding. *J Clin Endocrinol Metabol* 2017;102:2974-2984.
3. Kohli R, Bradley D, Setchell KD, Eagon JC, Abumrad N, Klein S. Weight loss induced by Roux-en-Y gastric bypass but not laparoscopic adjustable gastric banding increases circulating bile acids. *J Clin Endocrinol Metab* 2013;98:E708-E712.
4. Pierre JF, Martinez KB, Ye H, et al. Activation of bile acid signaling improves metabolic phenotypes in high-fat diet-induced obese mice. *Am J Physiol Gastrointest Liver Physiol* 2016;311:G286-G304.
5. Simonen M, Dali-Youcef N, Kaminska D, et al. Conjugated bile acids associate with altered rates of glucose and lipid oxidation after Roux-en-Y gastric bypass. *Obes Surg* 2012;22:1473-1480.
6. Patti ME, Houten SM, Bianco AC, et al. Serum bile acids are higher in humans with prior gastric bypass: potential contribution to improved glucose and lipid metabolism. *Obesity (Silver Spring)* 2009;17:1671-1677.
7. Ahmad NN, Pfalzer A, Kaplan LM. Roux-en-Y gastric bypass normalizes the blunted postprandial bile acid excursion associated with obesity. *Int J Obes (Lond)* 2013;37:1553-1559.
8. Manning S, Batterham RL. The role of gut hormone peptide YY in energy and glucose homeostasis: twelve years on. *Annu Rev Physiol* 2014;76:585-608.
9. Nannipieri M, Baldi S, Mari A, et al. Roux-en-Y gastric bypass and sleeve gastrectomy: mechanisms of diabetes remission and role of gut hormones. *J Clin Endocrinol Metab* 2013;98:4391-4399.
10. Bose M, Machineni S, Olivan B, et al. Superior appetite hormone profile after equivalent weight loss by gastric bypass compared to gastric banding. *Obesity (Silver Spring)* 2010;18:1085-1091.
11. Shin ED, Estall JL, Izzo A, Drucker DJ, Brubaker PL. Mucosal adaptation to enteral nutrients is dependent on the physiologic actions of glucagon-like peptide-2 in mice. *Gastroenterology* 2005;128:1340-1353.
12. Ryan KK, Tremaroli V, Clemmensen C, et al. FXR is a molecular target for the effects of vertical sleeve gastrectomy. *Nature* 2014;509:183-188.
13. Zhang Y, Lee FY, Barrera G, et al. Activation of the nuclear receptor FXR improves hyperglycemia and hyperlipidemia in diabetic mice. *Proc Natl Acad Sci USA* 2006;103:1006-1011.
14. Prawitt J, Abdelkarim M, Stroeve JH, et al. Farnesoid X receptor deficiency improves glucose homeostasis in mouse models of obesity. *Diabetes* 2011;60:1861-1871.
15. Watanabe M, Horai Y, Houten SM, et al. Lowering bile acid pool size with a synthetic farnesoid X receptor (FXR) agonist induces obesity and diabetes through reduced energy expenditure. *J Biol Chem* 2011;286:26913-26920.
16. Cipriani S, Mencarelli A, Palladino G, Fiorucci S. FXR activation reverses insulin resistance and lipid abnormalities and protects against liver steatosis in Zucker (fa/fa) obese rats. *J Lipid Res* 2010;51:771-784.
17. Ma K, Saha PK, Chan L, Moore DD. Farnesoid X receptor is essential for normal glucose homeostasis. *J Clin Invest* 2006;116:1102-1109.
18. Gonzalez FJ, Jiang C, Patterson AD. An intestinal microbiota-farnesoid X receptor axis modulates metabolic disease. *Gastroenterology* 2016;151:845-859.
19. Pathak P, Liu H, Boehme S, et al. Farnesoid X receptor induces Takeda G-protein receptor 5 cross-talk to regulate bile acid synthesis and hepatic metabolism. *J Biol Chem* 2017;292:11055-11069.
20. Chavez JA, Siddique MM, Wang ST, Ching J, Shayman JA, Summers SA. Ceramides and glucosylceramides are independent antagonists of insulin signaling. *J Biol Chem* 2014;289:723-734.
21. Jiang C, Xie C, Lv Y, et al. Intestine-selective farnesoid X receptor inhibition improves obesity-related metabolic dysfunction. *Nat Commun* 2015;6:10166. doi:10.1038/ncomms10166
22. Flynn CR, Albaugh VL, Cai S, et al. Bile diversion to the distal small intestine has comparable metabolic benefits to bariatric surgery. *Nat Commun* 2015;6:7715. doi:10.1038/ncomms8715
23. Asayama K, Okada Y, Kato K. Peroxisomal beta-oxidation in liver and muscles of gold-thioglucose-induced obese mice: correlation with body weight. *Int J Obes* 1991;15:45-49.
24. Caporaso JG, Kuczynski J, Stombaugh J, et al. QIIME allows analysis of high-throughput community sequencing data. *Nat Methods* 2010;7:335-336.
25. Lee CK, Herbold CW, Polson SW, et al. Groundtruthing next-gen sequencing for microbial ecology-biases and errors in community structure estimates from PCR amplicon pyrosequencing. *PLoS One* 2012;7:e44224. doi:10.1371/journal.pone.0044224
26. Parks DJ, Blanchard SG, Bledsoe RK, et al. Bile acids: natural ligands for an orphan nuclear receptor. *Science* 1999;284:1365-1368.
27. Sinal CJ, Tohkin M, Miyata M, Ward JM, Lambert G, Gonzalez FJ. Targeted disruption of the nuclear receptor FXR/BAR impairs bile acid and lipid homeostasis. *Cell* 2000;102:731-744.
28. Montagner A, Polizzi A, Fouche E, et al. Liver PPARalpha is crucial for whole-body fatty acid homeostasis and is protective against NAFLD. *Gut* 2016;65:1202-1214.
29. Goncalves D, Barataud A, De Vadder F, et al. Bile routing modification reproduces key features of gastric bypass in rat. *Ann Surg* 2015;262:1006-1015.
30. Mottillo EP, Bloch AE, Leff T, Granneman JG. Lipolytic products activate peroxisome proliferator-activated receptor (PPAR) alpha and delta in brown adipocytes to match fatty acid oxidation with supply. *J Biol Chem* 2012;287:25038-25048.
31. Bijsmans IT, Guercini C, Ramos Pittol JM, et al. The glucocorticoid mometasone furoate is a novel FXR ligand that decreases inflammatory but not metabolic gene expression. *Sci Rep* 2015;5:14086. doi:10.1038/srep14086
32. Hao H, Cao L, Jiang C, et al. Farnesoid X receptor regulation of the NLRP3 inflammasome underlies cholestasis-associated sepsis. *Cell Metab* 2017;25:856-867.
33. Li F, Jiang C, Krausz KW, et al. Microbiome remodelling leads to inhibition of intestinal farnesoid X receptor signalling and decreased obesity. *Nat Commun* 2013;4:2384. doi:10.1038/ncomms3384
34. Schmitt J, Kong B, Stieger B, et al. Protective effects of farnesoid X receptor (FXR) on hepatic lipid accumulation are mediated by hepatic FXR and independent of intestinal FGF15 signal. *Liver Int* 2015;35:1133-1144.
35. Schittenhelm B, Wagner R, Kahny V, et al. Role of FXR in beta-cells of lean and obese mice. *Endocrinology* 2015;156:1263-1271.
36. Trabelsi MS, Daoudi M, Prawitt J, et al. Farnesoid X receptor inhibits glucagon-like peptide-1 production by enteroendocrine L cells. *Nat Commun* 2015;6:7629. doi:10.1038/ncomms8629
37. Friedman ES, Li Y, Shen TD, et al. FXR-dependent modulation of the human small intestinal microbiome by the bile acid derivative obeticholic acid. *Gastroenterology* 2018;155:1741-1752.
38. Carvalho FA, Koren O, Goodrich JK, et al. Transient inability to manage proteobacteria promotes chronic gut inflammation in TLR5-deficient mice. *Cell Host Microbe* 2012;12:139-152.
39. Nagata N, Xu L, Kohno S, et al. Glucoraphanin ameliorates obesity and insulin resistance through adipose tissue browning and reduction of metabolic endotoxemia in mice. *Diabetes* 2017;66:1222-1236.
40. Labbe A, Ganopolsky JG, Martoni CJ, Prakash S, Jones ML. Bacterial bile metabolising gene abundance in Crohn's, ulcerative colitis and type 2 diabetes metagenomes. *PLoS One* 2014;9:e115175. doi:10.1371/journal.pone.0115175
41. Gerard P. Metabolism of cholesterol and bile acids by the gut microbiota. *Pathogens* 2013;3:14-24.
42. Fukiya S, Arata M, Kawashima H, et al. Conversion of cholic acid and chenodeoxycholic acid into their 7-oxo derivatives by Bacteroides intestinalis AM-1 isolated from human feces. *FEMS Microbiol Lett* 2009;293:263-270.
43. Ma Y, Huang Y, Yan L, Gao M, Liu D. Synthetic FXR agonist GW4064 prevents diet-induced hepatic steatosis and insulin resistance. *Pharm Res* 2013;30:1447-1457.
44. Mudaliar S, Henry RR, Sanyal AJ, et al. Efficacy and safety of the farnesoid X receptor agonist obeticholic acid in patients with type 2 diabetes and nonalcoholic fatty liver disease. *Gastroenterology* 2013;145:574-582.
45. Sayin SI, Wahlstrom A, Felin J, et al. Gut microbiota regulates bile acid metabolism by reducing the levels of tauro-beta-muricholic acid, a naturally occurring FXR antagonist. *Cell Metab* 2013;17:225-235.